HHS Public Access

Author manuscript

J Alzheimers Dis. Author manuscript; available in PMC 2020 July 24.

Published in final edited form as:

J Alzheimers Dis. 2019 ; 70(4): 1259–1274. doi:10.3233/JAD-180678.

5xFAD mice display sex-dependent inflammatory gene induction during the prodromal stage of Alzheimer's disease

Zahra Manji, **Asheebo Rojas**, **Wenyi Wang**, **Raymond Dingledine**, **Nicholas H. Varvel***, **Thota Ganesh***

Department of Pharmacology and Chemical Biology, Emory University School of Medicine, 1510 Clifton Road, Atlanta, GA 30322

Abstract

Alzheimer's disease (AD) pathology consists of extracellular deposits of amyloid-β peptides (Aβ) and intracellular neurofibrillary tangles. These pathological alterations are accompanied by a neuroinflammatory response consisting of increased expression of inflammatory mediators. An anti-inflammatory strategy designed to prevent or delay the development of AD would benefit from knowing when neuroinflammation appears in the transgenic models during prodromal disease stages relative to Aβ pathology. We investigated the expression patterns of inflammatory mediators in the brain of 5xFAD mice in comparison to development of Aβ deposition. Expression changes in inflammatory mediators and glial markers are more robust in female mice starting at three months of age, in contrast to males in which there is no clear trend through five months. Female and male 5xFAD mice also displayed an age-dependent increase in cortical Aβ deposition congruent with neuroinflammation. Thus, in the 5xFAD mouse model of AD, administration of an anti-inflammatory agent would be most efficacious when administered before three months of age.

Keywords

cytokines; chemokines; amyloid; inflammation; Alzheimer's disease

Introduction

Alzheimer's disease (AD) is an increasingly prevalent, progressive neurodegenerative disorder that is the leading cause of dementia in the elderly. Approximately 44 million people suffer from dementia worldwide, and by 2050 this number is predicted to triple due to population aging, further exacerbating the socioeconomic burden of this neurological condition [1]. A definite diagnosis of AD requires post-mortem demonstration of deposition of amyloid-β (Aβ) peptides in senile plaques and neurofibrillary tangles (NFTs) in the brain parenchyma. Accompanying these hallmark pathological features are neuronal loss and a robust neuroinflammatory response [2].

*For correspondence, please contact: Dr. Nicholas H. Varvel: 404-727-7393; fax: 404-727-5635; nvarvel@emory.edu or Dr. Thota Ganesh, Phone: 404-727-7393; fax: 404-727-0365; tganesh@emory.edu.

Author contributions:

T.G. conceived and designed the study. Z.M., A.R., W.W., N.H.V. and T.G. performed the experiments. Z.M., A.R., R.D., and N.H.V. participated in data analysis. Z.M., A.R., R.D., N.H.V., and T.G. wrote the manuscript.

There is strong evidence for a direct involvement of neuroinflammatory processes in AD pathophysiology. First, increased numbers of inflammatory cells (microglia and astrocytes), especially in the immediate vicinity of Aβ deposits, and molecules such as cytokines, chemokines, and complement proteins are encountered in the AD brain [3]. Second, genetically modified mouse models have convincingly demonstrated a role for various inflammatory pathways in altering microglial activation and Aβ deposition including chemokines [4–6], nitric oxide synthase 2 [7], transforming growth factor beta (TGFβ) [8, 9], complement [10, 11], interleukin 1 beta (IL-1β) [12], and interleukin 10 (IL-10) [13, 14]. Finally, genetic variants in genes encoding inflammatory molecules elevate AD risk [15–19], suggesting altered inflammatory responses can promote AD.

Retrospective epidemiological studies have shown marked reduction in AD risk in patient populations treated with non-steroidal anti-inflammatory drugs (NSAIDs) [20, 21]. Unfortunately, prospective clinical trials enrolling AD patients suffer from mixed success [22–24], with the most recent data indicating no reduction in the progression of AD [25]. The reasons for these discordant outcomes remain unclear. However, it is possible that in the prospective studies with NSAID treatment was too short in duration, as retrospective epidemiological studies have reported that protective effects of NSAIDs are only encountered in individuals who have been taking NSAIDs for more than five years [26]. Alternatively, NSAID treatment might have been initiated too late in the disease process to be effective [27].

Here we investigated the gene expression changes of multiple inflammatory analytes in AD-relevant brain regions as a function of age during the earliest stages of congophilic Aβ deposition in the widely utilized 5xFAD mouse model of AD on a congenic C57BL/6 inbred genetic background. Previous studies have utilized 5xFAD on an F1 hybrid background [28, 29]. To achieve desired statistical power we focused our analysis on nine inflammatory analytes known to be elevated in human AD brain tissue [30]. The chemokine C-X-C motif ligand 10 (CXCL10) was the earliest inflammatory mediator induced at three months of age, and this was only observed in the female brain. Transcripts of pro-inflammatory cytokines IL-1β, interleukin 6 (IL-6), tumor necrosis factor (TNFα) and chemokines C-C motif ligand 2 (CCL2) and CXCL10 were significantly induced in five-month-old female 5xFAD brain compared to nontransgenic littermates, and COX-2 protein was elevated in five month old female 5xFAD mice. In contrast, only TNFα and COX-2 mRNAs showed significant upregulation in male 5xFAD, and this was limited to the five and four month time points, respectively. These findings give insight into the temporal changes in inflammatory gene expression during the early stages of amyloid pathology in the congenic C57BL/6 5xFAD mouse model of AD. Furthermore, this information can aid in the design and execution of pre-clinical trials in mice targeting inflammation at the earliest stages of AD progression.

Materials and Methods

Mice

All procedures and experiments concerning animals were approved by Emory University Institutional Animal Care and Use Committee and conformed to NIH guidelines. Mice were housed under a 12-hour light/dark cycle with food and water *ad libitum*. 5xFAD mice

(MMRRC stock number: 34848-JAX) [31] were originally created on a mixed B6/SJL genetic background. We maintain the 5xFAD line on a congenic C57BL/6 (Charles River) background by repeated backcrossing over ten generations. Female and male mice hemizygous for the transgene were used. Nontransgenic littermates (labeled as “WT” controls in the text and figures) were housed in the same manner as 5xFAD mice and used for comparison.

Tissue Processing

5xFAD mice and age-matched nontransgenic controls were deeply anesthetized with isoflurane and their brains rapidly removed from the cranium. The brain was immediately bisected through the midline, and one hemisphere was fixed for 24 hours in 4% (wt/vol) paraformaldehyde at 4°C for Congo red staining and immunohistochemistry. For one cohort, the hemi-brains minus the cerebellum were separated and frozen on dry ice for RNA isolation. For the other cohort, the hippocampus and cortex were dissected from the other half of the brain, immediately frozen on dry ice and stored at −80°C for RNA isolation.

qRT-PCR.

Total RNA from mouse hemi-brain or cortex was isolated and purified by using TRIzol (Invitrogen) with the PureLink RNA Mini Kit (Invitrogen). RNA concentration and purity were estimated by the A260 value and A260/A280 ratio, respectively. First-strand cDNA synthesis was performed with 1 μg of total RNA, using qScript cDNA SuperMix (Quanta Biosciences) in a reaction volume of 20 μL at 25°C for five minutes, then 42°C for 30 minutes. The reaction was terminated by heating at 85°C for five minutes. Quantitative real-time polymerase chain reaction (qRT-PCR) was performed with technical duplicates by using 8 μL of 50x-diluted cDNA, 0.4 μM of primers, and iQ SYBR Green Supermix (Quanta Biosciences), with a final volume of 20 μL, in the iQ5 Multicolor Real-Time PCR Detection System (Bio-Rad). Cycling conditions were as follows: 95°C for two minutes followed by 40 cycles of 95°C for 15 seconds and then 60°C for one minute. Melting curve analysis was used to verify single-species PCR product. Fluorescence data were acquired at the 60°C step. Glyceraldehyde 3-phosphate dehydrogenase (GAPDH) was used as the internal control for relative quantification (Table 1). Samples without cDNA served as the negative controls. We also examined efficiency of the PCR reaction by determining the Ct values for serial dilutions of our cDNA and plotting the resulting Ct values as a function of the negative (log dilution factor). Analysis of quantitative real time PCR was performed by subtracting the cycle threshold (Ct) value of the internal control GAPDH from the measured Ct value obtained from the log phase of each amplification curve of each gene of interest. The fold increase of each gene of interest was estimated for each 5XFAD mouse relative to the amount of RNA found in the control animals using the $2^{-\Delta\Delta Ct}$ method [32]. All conditions for qRT-PCR were the same. Real time PCR primer sequences are listed in Table 1. Of the 9 inflammatory mediators investigated, three (IL-1β, IL-6 and TNFα) are produced and secreted by cells involved in both innate and acquired immunity to stimulate inflammation; two (CCL2 and CXCL10) are chemokines that recruit cells to sites of inflammation or injury. Glial fibrillary acidic protein (GFAP) and ionized calcium-binding adapter molecule 1 (Iba1) are glial markers of astrocytes and myeloid cells, respectively. Cyclooxygenase 2

(COX-2) is an intracellular enzyme that forms prostanoids and EP2 is a G-protein coupled receptor that is activated by prostaglandin E2. Both COX-2 and EP2 are immunomodulatory.

Immunohistochemistry and Congo Red Staining

The fixed brain tissue was cyroprotected in 30% sucrose in phosphate buffered saline (PBS). Brains were subsequently frozen in 2-methylbutane and sagittally (females) or coronally (males) sectioned at 30 μm using a cryostat or microtome. Immunohistochemical stains were performed using Vectastain Elite ABC kits (Vector Laboratories), according to a recently described protocol [33]. The primary antibodies used included a rabbit polyclonal antibody to Iba1 (Wako, 019–19741, 1:1000 dilution), a rabbit polyclonal to COX-2 (Abcam, ab15191; 1:1000 dilution) and a mouse monoclonal to human APP/Aβ (Biolegend, clone 6E10, 1:1000 dilution). Congo red staining was performed according to standard laboratory procedures. Images were acquired on an Axioplan 2 microscope with an attached AxioCam MRm camera, using a 2x/0.5 air objective lens and AxioVision 4.7 software (all from Carl Zeiss). Every 12th section (30 μm) through the entire neocortex was assessed for Aβ load. Analysis was performed using the Stereologer software (Stereo Investigator 6 MBF Bioscience) and a motorized x-y-z stage coupled to a video microscopy system (Microfire color microscope camera; Optronics). Congophilic amyloid load was analyzed using the area fraction technique [34, 35].

Confocal stacks (1 μm) were obtained from 30 μm coronal brain sections stained to identify Iba1, COX-2 and APP/Aβ with a multiphoton Leica SP8 MP microscope. Stacks were subsequently analyzed with Imaris 6.4.0 (Bitplane). Analysis was restricted to regions that displayed a robust and consistent staining intensity and revealed fine details of the microglia processes. The surface of the cells and Aβ deposits were reconstructed using Imaris.

COX-2 Western Blot

In a separate cohort of mice cerebral cortices from five-month-old female and male 5xFAD mice and age- and sex-matched littermate wild-type mice were homogenized in RIPA buffer containing protease and phosphatase inhibitors (Thermo Scientific). Brain homogenates were subsequently sonicated to shear DNA and centrifuged at 14,000 × g for 30 minutes at 4 ° C to remove cell debris. The amount of total protein was measured by a Bradford protein assay. Total protein was separated on a gradient (4–20%) Mini-PROTEAN TGX Gel and electroblotted onto Polyvinylidene fluoride (PVDF) membranes (Millipore). Membranes were blocked for 6 h at 4 °C with Odyssey blocking solution (Li-Cor), then incubated overnight at 4 ° C with primary antibodies for COX-2 (1:1000, Abcam) and GAPDH (1:10,000, Calbiochem), followed by incubation with polyclonal IRDye secondary antibodies 680LT and 800CW (1:15,000, Li-Cor). The blots were imaged using a ChemiDoc MP Imaging System (Bio-Rad). The ratio of COX-2 to GAPDH was determined for each sample and the average COX-2 level for each group was compared using a Student's *t*-test.

COX-2 ELISA

The same cortical homogenates utilized for Western blot analysis were examined for total COX-2 by ELISA (LifeSpan BioSciences) according to manufacturer's protocol.

Data and Statistical Analysis

Data are presented as mean ± standard error. Statistical analysis was performed using GraphPad Prism version 6 (GraphPad Software). Two-way ANOVA (genotype × age) was used for comparison of the mean ΔΔCt values between 5xFAD mice and non-transgenic, age- and gender-matched littermate controls at each time point with Sidak correction for multiple comparisons. Statistical outliers were identified by Grubb's test and removed just prior to statistical analysis. The ΔΔCt values were converted to fold change for data presentation. For all analyses, the differences were considered to be statistically different if $p<0.05$.

Results

Expression of inflammatory genes in male and female 5xFAD mice.

The 5xFAD transgenic mouse model of AD expresses mutant human amyloid precursor protein (*APP*) harboring the Swedish (K670N, M671L), Florida (I716V), and London (V717I) familial Alzheimer's disease (FAD) mutations expressed by the Thy1 promoter, as well as mutant human presenilin 1 (*PSEN1*) harboring two FAD mutations, M146L and L286V, also driven by the Thy1 promoter [31]. The 5xFAD mouse maintained on the B6/SJL genetic background begins to develop Aβ deposition at two months of age in the deep cortical layers and subiculum [31]. With aging, Aβ deposition is observed throughout the cortex, hippocampus, thalamus, brainstem, and olfactory bulb. Accompanying Aβ deposition is an inflammatory response typified by astrogliosis and microgliosis [31].

To determine the earliest changes in inflammatory gene expression in the 5xFAD model on a congenic C57BL/6 genetic background, cohorts of male and female 5xFAD mice were sacrificed at monthly intervals between one and five months of age inclusive. Age- and gender-matched, non-transgenic littermates were sacrificed in parallel, hereafter simply referred to as "wildtype (WT)". Quantitative real-time PCR (qRT-PCR) was performed on mRNA extracted from hemi-brains (minus cerebellum).

Cytokines—In male 5xFAD mice, IL-1β mRNA levels in the brain were decreased by >50% at two and three months of age when compared to WT control mice, but then rose back to a level similar to WT controls at four and five months of age (Figure 1). The mRNA levels of TNFα were decreased by ~50% in 5xFAD male brains at two months of age and elevated by 1.8 fold over WT at five months of age. The brain levels of IL-6 in 5xFAD male mice were not significantly different from WT at any time point examined (Figure 1). Female mice showed a more vigorous inflammatory response as described below.

In female 5xFAD mice mRNA levels of IL-1β were significantly lower than WT at one month of age and elevated 2.4 fold over WT at the five-month time point (Figure 1). The mRNA levels of TNFα were elevated in female 5xFAD brain at three months of age by 1.8 fold and at five months of age by 2.6 fold, but were similar to WT at one and four months of age and decreased in 5xFAD brain at two months of age (Figure 1). In contrast to male 5xFAD wherein no change in IL-6 mRNA levels were detected, in female 5xFAD mice IL-6 levels were only significantly different than WT at two and three months of age (Figure 1).

Chemokines—The mRNA of chemokines, CCL2 and CXCL10, were also investigated in male and female 5xFAD mice as well as age- and gender-matched, non-transgenic WT. Hemi-brain levels of mRNA for both CCL2 and CXCL10 were not different between male 5xFAD and WT at the time points examined (Figure 2). In female mice by contrast, CCL2 mRNA was elevated 2.3 fold in five-month-old 5xFAD mice over WT. CXCL10 displayed an age-dependent increase in female 5xFAD mice. CXCL10 levels were increased 3.2 fold in female 5xFAD brain at three months of age, and was further elevated to 8.7 fold in five-month-old 5xFAD compared to WT littermates (Figure 2).

Glial Markers—The level of GFAP and Iba1 mRNAs was not different in male 5xFAD mice compared to WT up to five months of age (Figure 3). However, significant increases were encountered in GFAP and Iba1 mRNA in female 5xFAD mice. GFAP mRNAs in 5xFAD brain were increased 2.9 fold over WT at three months, 7.1 fold at four months, and 3 fold at five months of age. There was an age-dependent increase in the mRNA of Iba1 in 5xFAD mice. However, the elevation of Iba1 mRNA was more gradual beginning at three months of age and was significantly induced at five months with a maximum 2-fold induction (Figure 3).

COX-2 and EP2—The induction of the immediate early gene, cyclooxygenase-2 (COX-2), and the immunomodulatory prostanoid receptor, EP2, was evaluated in hemibrains from 5xFAD male and female mice. COX-2 mRNA levels were increased 2-fold in males at 4 months of age, and 1.6-fold at three months of age in females, but were not different from WT levels at the other time points examined (Figure 4). The EP2 levels were slightly suppressed in 5xFAD male brain at 2–3 months, but not different from WT mice at 4–5 months, whereas the female 5xFAD brain mice showed slightly reduced levels at 1 month, and were elevated 1.6 fold in brain from three-month-old mice (Figure 4).

Assessment of inflammatory mediator mRNA levels in the cortex of female 5xFAD mice

To determine whether the changes in inflammatory gene expression were also observed in isolated cortex, qRT-PCR analysis was performed on mRNA extracted from cortices obtained from a different cohort of female mice as females consistently displayed an earlier and greater induction of inflammatory mediators examined over controls compared to male 5xFAD mice (Figures 1–4). We chose to focus on the cortex as it represented the greatest individual tissue mass of the hemi-brain and in the 5xFAD model Aβ deposition is identified earliest in the deep cortical layers [31].

Cortices from cohorts of female 5xFAD and age- and gender matched non-transgenic mice aged to one, three, and five months of age were collected. Cortical levels of cytokines IL-1β, IL-6, and TNFα were elevated over WT at five months, but not at one or three months of age (Figure 5A–C). Cortical levels of CXCL10 were first elevated by 2.2 fold at three months of age and reached nearly 8 fold expression over WT at the five-month time point (Figure 5D). CCL2 levels were elevated about two fold in cortex from five month old 5xFAD mice, but CCL2 mRNA levels were indistinguishable from WT at earlier time points (Figure 5E). - The mRNA levels of GFAP were elevated 4-fold at the five month time point (Figure 5F), but the mRNA levels of Iba1 (Figure 5G), COX-2 (Figure 5H), and EP2 (Figure 5I) in

5xFAD cortex were not significantly different from non-transgenic WT littermates at the time points examined. Note that cortical levels of mRNA for all inflammatory mediators in female 5xFAD mice mimicked their expression patterns in the female hemi-brain, especially at 5-months of age.

COX-2 protein levels are elevated in the cortex of female 5xFAD mice, but not in male 5xFAD mice

Western blot was performed using cortical homogenates from five-month-old female 5xFAD mice and age- and sex-matched wild type littermates to examine COX-2 protein levels. Elevated COX-2 protein was detected in 5xFAD mice when compared to age-matched littermates (Figure 6A) with the average ratio of COX-2/GAPDH over 2-fold greater in the 5xFAD mice (Figure 6B) indicating that the presence of the 5xFAD transgene causes induction of COX-2 expression in cortical tissue. ELISA was performed as a secondary measure of the level of COX-2 in the same protein homogenates used for western blot. Like western blot, ELISA revealed a significantly higher level of COX-2 protein in the cortex of female 5xFAD mice at 5 months of age (Figure 6C). Immunohistochemistry was performed on brain sections from wild-type and 5xFAD mice to determine whether the increased COX-2 protein is associated with Aβ plaque formation. In wild-type female mice at five months of age COX-2 immunoreactive cells with small cell bodies and thin processes were observed tiled throughout subcortical brain regions, the hippocampus and cortex, however no Congo red staining was encountered (Figure 6D, upper panel). In contrast, age-matched 5xFAD female mice had numerous Congo red-positive plaques throughout the cortex, and COX-2 immunoreactive cells were localized in close proximity to the Aβ deposits (Figure 6D, lower panel). Non-plaque-associated COX-2 immunoreactive cells were also observed tiled throughout all brain regions, and these cells had nearly the same morphology as the COX-2-positive cells encountered in the wild-type mice. Computer-assisted image analysis and 3D surface reconstruction of Iba1-labeled innate immune myeloid cells were performed to determine whether the COX-2-immunopositive cells were myeloid cells (Figure 6E). COX-2 immunostaining was co-localized to cortical Iba1-positive cells that were both plaque-associated and non-plaque-associated (Figure 6E).

To determine if male 5xFAD mice also upregulate COX-2 in the cortex, western blot was performed using cortical homogenates from five-month-old male 5xFAD mice and age- wild type male littermates. In contrast to five-month-old female 5xFAD mice, male 5xFAD mice did not show elevated COX-2 protein compared to age- and sex-matched littermates (Figure 6F). The average ratio of COX-2/GAPDH was nearly the same in male 5xFAD and non-transgenic mice (Figure 6G).

Histological examination of cortical amyloid deposition

To examine the amyloid load in the cortex of female 5xFAD mice, brain tissue sections were stained for congophilic Aβ deposits with the amyloid stain, Congo red. Examination of brain sections from female animals sacrificed at one month of age revealed no cortical congophilic Aβ deposits (Figure 7A). In contrast, Congo red-positive Aβ deposits were apparent in the cortex from three-month-old female 5xFAD mice (Figure 7B), and the congophilic amyloid load was further increased at the five month time point (Figure 7C). Analysis of cortical area

covered by congophilic Aβ deposition as a quantitative measure revealed that dense-core Aβ deposition is present at three months of age and further increases from three to five months of age (Figure 7D).

Analysis of the amyloid burden in brain sections obtained from the cortex of male 5xFAD mice likewise showed no Congo red-positive plaques at one month of age (Figure 7E), however, Aβ deposits were observed in male 5xFAD at three (Figure 7F) and five months of age (Figure 7G). Quantification of the cortical area occupied by congophilic Aβ staining revealed a similar increasing trend of Aβ deposition in male and female 5xFAD (Figure 7H), although the amyloid burden was higher in female mice at each age.

Discussion

Elevated inflammation can have a profound impact on AD pathogenesis [2], and it has been proposed that chronic microglial activation might exacerbate Aβ plaque pathology and enhance the development of neurofibrillary tangles (NFTs), possibly through elevated expression and secretion of inflammatory mediators [36]. Thus, identifying the earliest inflammatory changes in a widely used mouse model of AD will be of interest for the future development of strategies and validation of therapeutics in preclinical mouse studies targeting inflammation in AD.

The 5xFAD mouse model of AD was initially created on C57BL6/SJL background and is widely used to study age-dependent progression in AD-like pathology [31]. Subsequently, the hybrid 5xFAD mouse line was backcrossed to the inbred C57BL/6 mouse strain to create a congenic line [37, 38]. In the current studies, the congenic 5xFAD mouse on the inbred C57BL/6 background was utilized. Female transgenic mouse models of AD typically have earlier onset of Aβ pathology than their male transgenic counterparts [39–41]. Moreover, behavioral deficits are also more severe in female transgenic mice [42–44]. Hormonal differences between males and females [45] and even hormonal levels during development [46] are possible reasons for sex-dependent risk of AD. Here, we performed longitudinal studies on male and female 5xFAD mice to determine the temporal profile of inflammatory mediator induction in AD-relevant brain regions. The induction of inflammatory mediators was determined by normalizing mRNA changes in 5xFAD mice to age- and gender-matched non-transgenic littermate wild-type mice at each time-point examined. Notably, our results reveal that female 5xFAD mice display an earlier and more robust induction of inflammatory mediators than male 5xFAD, which is in agreement with previous findings revealing sex differences in the inflammatory profile in 5xFAD mice [47].

Normal aging is typified by heightened inflammation. Elevated numbers of innate and adaptive immune cells in the blood and circulating cytokines are encountered in elderly individuals [48–51]. Elevated levels of C-reactive protein, IL-6, and IL-10 were inversely correlated with executive performance on neuropsychological tests [52]. Interestingly, a number of behavioral disorders such as clinical depression, chronic pain, and fatigue are over-represented by women, and there are clear differences in the immune response in men and women [53]. Nevertheless, it remains unclear if altered age-related inflammation is the critical factor in elevating AD risk in women.

The earliest inflammatory mediator elevated in 5xFAD mice was the chemokine CXCL10. CXCL10 was significantly upregulated in the brain and cortex of female, but not male 5xFAD mice beginning at 3 months (Figure 2). Notably, previous studies have reported a positive correlation between CXCL10 in the cerebrospinal fluid (CSF) and cognitive impairment in AD patients [54, 55]. In AD mouse models, expression of CXCL10 is encountered in close proximity to Aβ deposits [56]. Interestingly, genetic elimination of chemokine receptor CXCR3, the primary receptor for CXCL10, in a mouse model of AD reduced Aβ deposition, decreased inflammatory cytokines, and attenuated behavioral deficits [6], highlighting the potential beneficial effects of quenching CXCR3-CXCL10 signaling before AD symptoms appear.

Another chemokine elevated in female 5xFAD brain, but not male 5xFAD brain, was CCL2. Earlier reports indicate that serum CCL2 levels are elevated in patients with mild but not severe AD [57], and CCL2 is elevated in cerebrospinal fluid early in disease progression [54], suggesting that CCL2 might be important in early AD pathogenesis, The primary receptor for CCL2 is CCR2, and CCR2 activation has been identified as a driver of peripheral monocyte recruitment to the inflamed and injured brain in multiple neurological conditions [33, 58]. Early reports indicated that peripheral cells were recruited to Aβ deposits in mouse models of the AD after irradiation and bone marrow chimerism [59]. However, more recent studies in a parabiosis model have failed to identify blood-borne immune cells surrounding Aβ deposits, arguing that innate immune cells clustering around Aβ deposits are derived from the brain resident microglial population [60]. Genetic ablation of CCR2 in AD mouse models resulted in enhanced Aβ pathology [4, 61], suggesting that blood-derived monocytes are recruited to the brain and are more proficient at Aβ clearance than brain-resident microglia, or exacerbate phagocytotic activity of resident microglia. However, ablation of resident microglia and repopulation of brain with peripheral monocytes was not sufficient to clear amyloid load [35, 62]. Taken together, these studies indicate that the extent and consequence of peripheral monocyte recruitment to the AD brain is not well understood.

The relationship between inflammatory cytokines and Aβ pathology has been examined in a number of studies. One of the earliest inflammatory changes in the human AD brain and Down's syndrome brain is IL-1β expression by microglia and astrocytes [63]. Interestingly, overexpression of the pro-inflammatory cytokine IL-1β by astrocytes reduced AD plaque pathology in a mouse model of the disease [12]. However, overexpression of IL-1β exacerbated tau pathology in the 3xTgAD mouse model of AD [64], indicating a dichotomous role for IL-1β in the evolution of AD pathology. Moreover, administration of an IL-1 receptor antagonist reduced tau pathology in the hTau transgenic mouse [65]. One mechanism for bioactive IL-1β production is by activation of the NOD-like receptor (NLR) family, pyrin domain containing 3 (NLRP3) inflammasome. Inactivation of NLRP3 in an AD mouse model reduces IL-1β, improves the clearance of Aβ, and ameliorates plaque pathology, culminating in protection from spatial memory loss [66]. Thus, the role of IL-1β in AD pathogenesis is complex and this complexity might reflect differential action of IL-1β during various stages of disease progression, initially protective but then deleterious if chronic.

In addition to IL-1β, the involvement of TNFα in AD has also been examined. Elevated TNFα is associated with the induction of acute as well as chronic inflammation [67]. TNFα is elevated in AD patient plasma [68]. Two functional forms of TNFα exist, soluble TNFα (sTNFα) and transmembrane TNFα (tmTNFα), and each has distinct bioactivities. Notably, specifically inhibiting sTNFα was protective in the 5xFAD mouse model, resulting in reduced amyloid deposition in the hippocampus, reduced trafficking of peripheral leukocytes to the brain, and rescued long-term potentiation (LTP), highlighting the value of targeting sTNFα in AD or limiting TNFα gene induction as a viable therapy [69]. Our finding that TNFα mRNA in the brain is increased in female 5xFAD mice at 3 and 5 months of age coincides with a 45% increase in cortical area covered by congophillic amyloid.

Neuronal COX-2 levels are greater in AD brain than in non-AD brain tissue [70, 71]. During early Braak stages the density of COX-2-positive neurons is elevated over nondemented controls, yet the density of COX-2 immunoreactive neurons decreases in advanced Braak stages [72]. Here, we demonstrate that both COX-2 and EP2 expression was elevated in the hemi-brains of female mice at 3-months of age when Aβ plaques are forming (Figure 7). Unfortunately, prospective clinical trials utilizing NSAIDs have had discordant clinical outcomes [22–24]. On the other hand, more specific downstream targets such as the prostaglandin EP2 receptor may be beneficial for reducing neuroinflammation in AD, as EP2 antagonism has shown to be effective at quenching brain inflammation after status epilepticus in rodents [73, 74]. In an epilepsy context EP2 appears to mediate most of the deleterious consequences of COX-2 induction [75, 76]. It will be important to investigate whether novel small molecule anti-inflammatory agents can reverse the expression profile of these inflammatory mediators in 5xFAD mice and display a disease modifying effect in AD.

Both microglia and astrocytes are encountered in close proximity to dense core amyloid deposits in human AD brain [3]. There is a robust age-dependent increase in brain Iba1+ microglia and GFAP+ astrocytes in AD mouse models [35, 77, 78]. In the current study, we found an age-dependent increase in both GFAP and Iba1 transcripts in female 5xFAD brain. The elevated levels of GFAP and Iba1 transcripts could be attributed to increased expression within each cellular population and/or proliferation of astrocytes and microglia, as both populations proliferate in AD mouse models [34].

A recent study reported elevated levels of TNFα and CD45, but not CCL2, in the midbrain of six-month-old 5xFAD mice of mix-gender [69]. In the cortex of these same mice, CD45, but not TNFα and CCL2, was significantly elevated [69]. In both brain regions the data were compared to two-month-old non-transgenic mice. In contrast, in the present study we compared gene induction in 5xFAD mice at each time point to non-transgenic littermates, and this could account for the discordant findings.

In conclusion, we provide evidence that CXCL10 mRNA is induced early in the cortex of three-month old female 5xFAD mice, and is the first inflammatory mediator induced among the examined targets. Moreover, female 5xFAD mice showed an earlier and greater induction of multiple inflammatory mediators including CXCL10, CCL2, IL-1β, and TNFα as well as the astroglial marker GFAP and microglial marker Iba1. Although the temporal appearance of amyloid plaques was similar in male and female 5xFAD mice, plaque density

was greater in female mice, which is associated with the different inflammatory profiles. The current study using the 5xFAD mouse model of AD has revealed a temporal profile of the evolution of inflammatory gene induction changes during the earliest stages of Aβ deposition in both male and female mice in comparison to age- and gender matched non-transgenic littermate WT. These findings provide a valuable resource for future studies utilizing the widely used 5xFAD mouse model in the design and execution of pre-clinical trials designed to target inflammation at the earliest stages of AD progression.

Acknowledgements

This work was supported by ADDF grant 20131001 (T.G.) and NIH/NIA grant U01 AG052460 (T.G.). We thank Dr. Malu Tansey for the use of video microscopy system with motorized stage and Stereologer software quantification of amyloid load, and for providing a pair of 5xFAD mice on congenic C57BL/6 background for use in our studies. The authors also thank Dr. Allan Levey for his helpful technical assistance and Mrs. Laura Fox-Goharioon and Mr. William Giang at Cell Imaging Microscopy Core, for assistance with imaging.

References

[1]. Lane CA, Hardy J, Schott JM (2018) Alzheimer's disease. Eur J Neurol 25, 59–70. [PubMed: 28872215]

[2]. Ardura-Fabregat A, Boddeke E, Boza-Serrano A, Brioschi S, Castro-Gomez S, Ceyzeriat K, Dansokho C, Dierkes T, Gelders G, Heneka MT, Hoeijmakers L, Hoffmann A, Iaccarino L, Jahnert S, Kuhbandner K, Landreth G, Lonnemann N, Loschmann PA, McManus RM, Paulus A, Reemst K, Sanchez-Caro JM, Tiberi A, Van der Perren A, Vautheny A, Venegas C, Webers A, Weydt P, Wijasa TS, Xiang X, Yang Y (2017) Targeting Neuroinflammation to Treat Alzheimer's Disease. CNS Drugs 31, 1057–1082. [PubMed: 29260466]

[3]. Akiyama H, Barger S, Barnum S, Bradt B, Bauer J, Cole GM, Cooper NR, Eikelenboom P, Emmerling M, Fiebich BL, Finch CE, Frautschy S, Griffin WS, Hampel H, Hull M, Landreth G, Lue L, Mrak R, Mackenzie IR, McGeer PL, O'Banion MK, Pachter J, Pasinetti G, Plata-Salaman C, Rogers J, Rydel R, Shen Y, Streit W, Strohmeyer R, Tooyoma I, Van Muiswinkel FL, Veerhuis R, Walker D, Webster S, Wegrzyniak B, Wenk G, Wyss-Coray T (2000) Inflammation and Alzheimer's disease Neurobiol Aging 21, 383–421. [PubMed: 10858586]

[4]. El Khoury J, Toft M, Hickman SE, Means TK, Terada K, Geula C, Luster AD (2007) Ccr2 deficiency impairs microglial accumulation and accelerates progression of Alzheimer-like disease. Nat Med 13, 432–438. [PubMed: 17351623]

[5]. Lee S, Varvel NH, Konerth ME, Xu G, Cardona AE, Ransohoff RM, Lamb BT (2010) CX3CR1 deficiency alters microglial activation and reduces beta-amyloid deposition in two Alzheimer's disease mouse models. Am J Pathol 177, 2549–2562. [PubMed: 20864679]

[6]. Krauthausen M, Kummer MP, Zimmermann J, Reyes-Irisarri E, Terwel D, Bulic B, Heneka MT, Muller M (2015) CXCR3 promotes plaque formation and behavioral deficits in an Alzheimer's disease model. J Clin Invest 125, 365–378. [PubMed: 25500888]

[7]. Colton CA, Wilcock DM, Wink DA, Davis J, Van Nostrand WE, Vitek MP (2008) The effects of NOS2 gene deletion on mice expressing mutated human AbetaPP. J Alzheimers Dis 15, 571–587. [PubMed: 19096157]

[8]. Town T, Laouar Y, Pittenger C, Mori T, Szekely CA, Tan J, Duman RS, Flavell RA (2008) Blocking TGF-beta-Smad2/3 innate immune signaling mitigates Alzheimer-like pathology. Nat Med 14, 681–687. [PubMed: 18516051]

[9]. Wyss-Coray T, Lin C, Yan F, Yu GQ, Rohde M, McConlogue L, Masliah E, Mucke L (2001) TGF-beta1 promotes microglial amyloid-beta clearance and reduces plaque burden in transgenic mice. Nat Med 7, 612–618. [PubMed: 11329064]

[10]. Fonseca MI, Chu SH, Berci AM, Benoit ME, Peters DG, Kimura Y, Tenner AJ (2011) Contribution of complement activation pathways to neuropathology differs among mouse models of Alzheimer's disease. J Neuroinflammation 8, 4. [PubMed: 21235806]

[11]. Maier M, Peng Y, Jiang L, Seabrook TJ, Carroll MC, Lemere CA (2008) Complement C3 deficiency leads to accelerated amyloid beta plaque deposition and neurodegeneration and modulation of the microglia/macrophage phenotype in amyloid precursor protein transgenic mice. J Neurosci 28, 6333–6341. [PubMed: 18562603]

[12]. Shaftel SS, Kyrkanides S, Olschowka JA, Miller JN, Johnson RE, O'Banion MK (2007) Sustained hippocampal IL-1 beta overexpression mediates chronic neuroinflammation and ameliorates Alzheimer plaque pathology. J Clin Invest 117, 1595–1604. [PubMed: 17549256]

[13]. Chakrabarty P, Li A, Ceballos-Diaz C, Eddy JA, Funk CC, Moore B, DiNunno N, Rosario AM, Cruz PE, Verbeeck C, Sacino A, Nix S, Janus C, Price ND, Das P, Golde TE (2015) IL-10 alters immunoproteostasis in APP mice, increasing plaque burden and worsening cognitive behavior. Neuron 85, 519–533. [PubMed: 25619653]

[14]. Guillot-Sestier MV, Doty KR, Gate D, Rodriguez J Jr., Leung BP, Rezai-Zadeh K, Town T (2015) Il10 deficiency rebalances innate immunity to mitigate Alzheimer-like pathology. Neuron 85, 534–548. [PubMed: 25619654]

[15]. Guerreiro R, Wojtas A, Bras J, Carrasquillo M, Rogaeva E, Majounie E, Cruchaga C, Sassi C, Kauwe JS, Younkin S, Hazrati L, Collinge J, Pocock J, Lashley T, Williams J, Lambert JC, Amouyel P, Goate A, Rademakers R, Morgan K, Powell J, St George-Hyslop P, Singleton A, Hardy J, Alzheimer Genetic Analysis G (2013) TREM2 variants in Alzheimer's disease. N Engl J Med 368, 117–127. [PubMed: 23150934]

[16]. Jonsson T, Stefansson H, Steinberg S, Jonsdottir I, Jonsson PV, Snaedal J, Bjornsson S, Huttenlocher J, Levey AI, Lah JJ, Rujescu D, Hampel H, Giegling I, Andreassen OA, Engedal K, Ulstein I, Djurovic S, Ibrahim-Verbaas C, Hofman A, Ikram MA, van Duijn CM, Thorsteinsdottir U, Kong A, Stefansson K (2013) Variant of TREM2 associated with the risk of Alzheimer's disease. N Engl J Med 368, 107–116. [PubMed: 23150908]

[17]. Karch CM, Goate AM (2015) Alzheimer's disease risk genes and mechanisms of disease pathogenesis. Biol Psychiatry 77, 43–51. [PubMed: 24951455]

[18]. Hollingworth P, Harold D, Sims R, Gerrish A, Lambert JC, Carrasquillo MM, Abraham R, Hamshere ML, Pahwa JS, Moskvina V, Dowzell K, Jones N, Stretton A, Thomas C, Richards A, Ivanov D, Widdowson C, Chapman J, Lovestone S, Powell J, Proitsi P, Lupton MK, Brayne C, Rubinsztein DC, Gill M, Lawlor B, Lynch A, Brown KS, Passmore PA, Craig D, McGuinness B, Todd S, Holmes C, Mann D, Smith AD, Beaumont H, Warden D, Wilcock G, Love S, Kehoe PG, Hooper NM, Vardy ER, Hardy J, Mead S, Fox NC, Rossor M, Collinge J, Maier W, Jessen F, Ruther E, Schurmann B, Heun R, Kolsch H, van den Bussche H, Heuser I, Kornhuber J, Wiltfang J, Dichgans M, Frolich L, Hampel H, Gallacher J, Hull M, Rujescu D, Giegling I, Goate AM, Kauwe JS, Cruchaga C, Nowotny P, Morris JC, Mayo K, Sleegers K, Bettens K, Engelborghs S, De Deyn PP, Van Broeckhoven C, Livingston G, Bass NJ, Gurling H, McQuillin A, Gwilliam R, Deloukas P, Al-Chalabi A, Shaw CE, Tsolaki M, Singleton AB, Guerreiro R, Muhleisen TW, Nothen MM, Moebus S, Jockel KH, Klopp N, Wichmann HE, Pankratz VS, Sando SB, Aasly JO, Barcikowska M, Wszolek ZK, Dickson DW, Graff-Radford NR, Petersen RC, Alzheimer's Disease Neuroimaging I, van Duijn CM, Breteler MM, Ikram MA, DeStefano AL, Fitzpatrick AL, Lopez O, Launer LJ, Seshadri S, consortium C, Berr C, Campion D, Epelbaum J, Dartigues JF, Tzourio C, Alperovitch A, Lathrop M, consortium E, Feulner TM, Friedrich P, Riehle C, Krawczak M, Schreiber S, Mayhaus M, Nicolhaus S, Wagenpfeil S, Steinberg S, Stefansson H, Stefansson K, Snaedal J, Bjornsson S, Jonsson PV, Chouraki V, Genier-Boley B, Hiltunen M, Soininen H, Combarros O, Zelenika D, Delepine M, Bullido MJ, Pasquier F, Mateo I, Frank-Garcia A, Porcellini E, Hanon O, Coto E, Alvarez V, Bosco P, Siciliano G, Mancuso M, Panza F, Solfrizzi V, Nacmias B, Sorbi S, Bossu P, Piccardi P, Arosio B, Annoni G, Seripa D, Pilotto A, Scarpini E, Galimberti D, Brice A, Hannequin D, Licastro F, Jones L, Holmans PA, Jonsson T, Riemenschneider M, Morgan K, Younkin SG, Owen MJ, O'Donovan M, Amouyel P, Williams J (2011) Common variants at ABCA7, MS4A6A/MS4A4E, EPHA1, CD33 and CD2AP are associated with Alzheimer's disease. Nat Genet 43, 429–435. [PubMed: 21460840]

[19]. Naj AC, Jun G, Beecham GW, Wang LS, Vardarajan BN, Buros J, Gallins PJ, Buxbaum JD, Jarvik GP, Crane PK, Larson EB, Bird TD, Boeve BF, Graff-Radford NR, De Jager PL, Evans D, Schneider JA, Carrasquillo MM, Ertekin-Taner N, Younkin SG, Cruchaga C, Kauwe JS, Nowotny P, Kramer P, Hardy J, Huentelman MJ, Myers AJ, Barmada MM, Demirci FY, Baldwin CT, Green RC, Rogaeva E, St George-Hyslop P, Arnold SE, Barber R, Beach T, Bigio EH,

Bowen JD, Boxer A, Burke JR, Cairns NJ, Carlson CS, Carney RM, Carroll SL, Chui HC, Clark DG, Corneveaux J, Cotman CW, Cummings JL, DeCarli C, DeKosky ST, Diaz-Arrastia R, Dick M, Dickson DW, Ellis WG, Faber KM, Fallon KB, Farlow MR, Ferris S, Frosch MP, Galasko DR, Ganguli M, Gearing M, Geschwind DH, Ghetti B, Gilbert JR, Gilman S, Giordani B, Glass JD, Growdon JH, Hamilton RL, Harrell LE, Head E, Honig LS, Hulette CM, Hyman BT, Jicha GA, Jin LW, Johnson N, Karlawish J, Karydas A, Kaye JA, Kim R, Koo EH, Kowall NW, Lah JJ, Levey AI, Lieberman AP, Lopez OL, Mack WJ, Marson DC, Martiniuk F, Mash DC, Masliah E, McCormick WC, McCurry SM, McDavid AN, McKee AC, Mesulam M, Miller BL, Miller CA, Miller JW, Parisi JE, Perl DP, Peskind E, Petersen RC, Poon WW, Quinn JF, Rajbhandary RA, Raskind M, Reisberg B, Ringman JM, Roberson ED, Rosenberg RN, Sano M, Schneider LS, Seeley W, Shelanski ML, Slifer MA, Smith CD, Sonnen JA, Spina S, Stern RA, Tanzi RE, Trojanowski JQ, Troncoso JC, Van Deerlin VM, Vinters HV, Vonsattel JP, Weintraub S, Welsh-Bohmer KA, Williamson J, Woltjer RL, Cantwell LB, Dombroski BA, Beekly D, Lunetta KL, Martin ER, Kamboh MI, Saykin AJ, Reiman EM, Bennett DA, Morris JC, Montine TJ, Goate AM, Blacker D, Tsuang DW, Hakonarson H, Kukull WA, Foroud TM, Haines JL, Mayeux R, Pericak-Vance MA, Farrer LA, Schellenberg GD (2011) Common variants at MS4A4/MS4A6E, CD2AP, CD33 and EPHA1 are associated with late-onset Alzheimer's disease. Nat Genet 43, 436–441. [PubMed: 21460841]

[20]. McGeer PL, McGeer E, Rogers J, Sibley J (1990) Anti-inflammatory drugs and Alzheimer disease. Lancet 335, 1037.

[21]. in t' Veld BA, Ruitenberg A, Hofman A, Launer LJ, van Duijn CM, Stijnen T, Breteler MM, Stricker BH (2001) Nonsteroidal antiinflammatory drugs and the risk of Alzheimer's disease N Engl J Med 345, 1515–1521. [PubMed: 11794217]

[22]. Jaturapatporn D, Isaac MG, McCleery J, Tabet N (2012) Aspirin, steroidal and non-steroidal anti-inflammatory drugs for the treatment of Alzheimer's disease. Cochrane Database Syst Rev, CD006378.

[23]. Rogers J, Kirby LC, Hempelman SR, Berry DL, McGeer PL, Kaszniak AW, Zalinski J, Cofield M, Mansukhani L, Willson P, et al. (1993) Clinical trial of indomethacin in Alzheimer's disease. Neurology 43, 1609–1611. [PubMed: 8351023]

[24]. Breitner JC, Baker LD, Montine TJ, Meinert CL, Lyketsos CG, Ashe KH, Brandt J, Craft S, Evans DE, Green RC, Ismail MS, Martin BK, Mullan MJ, Sabbagh M, Tariot PN, Group AR (2011) Extended results of the Alzheimer's disease anti-inflammatory prevention trial. Alzheimers Dement 7, 402–411. [PubMed: 21784351]

[25]. Meyer PF, Tremblay-Mercier J, Leoutsakos J, Madjar C, Lafaille-Maignan ME, Savard M, Rosa-Neto P, Poirier J, Etienne P, Breitner J, group P-Ar (2019) INTREPAD: A randomized trial of naproxen to slow progress of presymptomatic Alzheimer disease. Neurology.

[26]. Vlad SC, Miller DR, Kowall NW, Felson DT (2008) Protective effects of NSAIDs on the development of Alzheimer disease. Neurology 70, 1672–1677. [PubMed: 18458226]

[27]. McGeer PL, McGeer EG (2007) NSAIDs and Alzheimer disease: epidemiological, animal model and clinical studies. Neurobiol Aging 28, 639–647. [PubMed: 16697488]

[28]. Landel V, Baranger K, Virard I, Loriod B, Khrestchatisky M, Rivera S, Benech P, Feron F (2014) Temporal gene profiling of the 5XFAD transgenic mouse model highlights the importance of microglial activation in Alzheimer's disease. Mol Neurodegener 9, 33. [PubMed: 25213090]

[29]. Devi L, Alldred MJ, Ginsberg SD, Ohno M (2010) Sex- and brain region-specific acceleration of beta-amyloidogenesis following behavioral stress in a mouse model of Alzheimer's disease. Mol Brain 3, 34. [PubMed: 21059265]

[30]. Heneka MT, Carson MJ, El Khoury J, Landreth GE, Brosseron F, Feinstein DL, Jacobs AH, Wyss-Coray T, Vitorica J, Ransohoff RM, Herrup K, Frautschy SA, Finsen B, Brown GC, Verkhratsky A, Yamanaka K, Koistinaho J, Latz E, Halle A, Petzold GC, Town T, Morgan D, Shinohara ML, Perry VH, Holmes C, Bazan NG, Brooks DJ, Hunot S, Joseph B, Deigendesch N, Garaschuk O, Boddeke E, Dinarello CA, Breitner JC, Cole GM, Golenbock DT, Kummer MP (2015) Neuroinflammation in Alzheimer's disease. Lancet Neurol 14, 388–405. [PubMed: 25792098]

[31]. Oakley H, Cole SL, Logan S, Maus E, Shao P, Craft J, Guillozet-Bongaarts A, Ohno M, Disterhoft J, Van Eldik L, Berry R, Vassar R (2006) Intraneuronal beta-amyloid aggregates,

neurodegeneration, and neuron loss in transgenic mice with five familial Alzheimer's disease mutations: potential factors in amyloid plaque formation. J Neurosci 26, 10129–10140. [PubMed: 17021169]

[32]. Livak KJ, Schmittgen TD (2001) Analysis of relative gene expression data using real-time quantitative PCR and the 2(-Delta Delta C(T)) Method. Methods 25, 402–408. [PubMed: 11846609]

[33]. Varvel NH, Neher JJ, Bosch A, Wang W, Ransohoff RM, Miller RJ, Dingledine R (2016) Infiltrating monocytes promote brain inflammation and exacerbate neuronal damage after status epilepticus. Proc Natl Acad Sci U S A 113, E5665–5674. [PubMed: 27601660]

[34]. Bondolfi L, Calhoun M, Ermini F, Kuhn HG, Wiederhold KH, Walker L, Staufenbiel M, Jucker M (2002) Amyloid-associated neuron loss and gliogenesis in the neocortex of amyloid precursor protein transgenic mice J Neurosci 22, 515–522. [PubMed: 11784797]

[35]. Varvel NH, Grathwohl SA, Degenhardt K, Resch C, Bosch A, Jucker M, Neher JJ (2015) Replacement of brain-resident myeloid cells does not alter cerebral amyloid-beta deposition in mouse models of Alzheimer's disease. J Exp Med 212, 1803–1809. [PubMed: 26458770]

[36]. Kitazawa M, Yamasaki TR, LaFerla FM (2004) Microglia as a potential bridge between the amyloid beta-peptide and tau. Ann N Y Acad Sci 1035, 85–103. [PubMed: 15681802]

[37]. Hillmann A, Hahn S, Schilling S, Hoffmann T, Demuth HU, Bulic B, Schneider-Axmann T, Bayer TA, Weggen S, Wirths O (2012) No improvement after chronic ibuprofen treatment in the 5XFAD mouse model of Alzheimer's disease. Neurobiol Aging 33, 833 e839–850.

[38]. Jawhar S, Trawicka A, Jenneckens C, Bayer TA, Wirths O (2012) Motor deficits, neuron loss, and reduced anxiety coinciding with axonal degeneration and intraneuronal Abeta aggregation in the 5XFAD mouse model of Alzheimer's disease. Neurobiol Aging 33, 196 e129–140.

[39]. Callahan MJ, Lipinski WJ, Bian F, Durham RA, Pack A, Walker LC (2001) Augmented senile plaque load in aged female beta-amyloid precursor protein-transgenic mice. Am J Pathol 158, 1173–1177. [PubMed: 11238065]

[40]. Gallagher JJ, Minogue AM, Lynch MA (2013) Impaired performance of female APP/PS1 mice in the Morris water maze is coupled with increased Abeta accumulation and microglial activation. Neurodegener Dis 11, 33–41. [PubMed: 22627185]

[41]. Hirata-Fukae C, Li HF, Hoe HS, Gray AJ, Minami SS, Hamada K, Niikura T, Hua F, Tsukagoshi-Nagai H, Horikoshi-Sakuraba Y, Mughal M, Rebeck GW, LaFerla FM, Mattson MP, Iwata N, Saido TC, Klein WL, Duff KE, Aisen PS, Matsuoka Y (2008) Females exhibit more extensive amyloid, but not tau, pathology in an Alzheimer transgenic model. Brain Res 1216, 92–103. [PubMed: 18486110]

[42]. Granger MW, Franko B, Taylor MW, Messier C, George-Hyslop PS, Bennett SA (2016) A TgCRND8 Mouse Model of Alzheimer's Disease Exhibits Sexual Dimorphisms in Behavioral Indices of Cognitive Reserve. J Alzheimers Dis 51, 757–773. [PubMed: 26890738]

[43]. King DL, Arendash GW, Crawford F, Sterk T, Menendez J, Mullan MJ (1999) Progressive and gender-dependent cognitive impairment in the APP(SW) transgenic mouse model for Alzheimer's disease. Behav Brain Res 103, 145–162. [PubMed: 10513583]

[44]. Melnikova T, Fromholt S, Kim H, Lee D, Xu G, Price A, Moore BD, Golde TE, Felsenstein KM, Savonenko A, Borchelt DR (2013) Reversible pathologic and cognitive phenotypes in an inducible model of Alzheimer-amyloidosis. J Neurosci 33, 3765–3779. [PubMed: 23447589]

[45]. Pike CJ, Carroll JC, Rosario ER, Barron AM (2009) Protective actions of sex steroid hormones in Alzheimer's disease. Front Neuroendocrinol 30, 239–258. [PubMed: 19427328]

[46]. Carroll JC, Rosario ER, Kreimer S, Villamagna A, Gentzschein E, Stanczyk FZ, Pike CJ (2010) Sex differences in beta-amyloid accumulation in 3xTg-AD mice: role of neonatal sex steroid hormone exposure. Brain Res 1366, 233–245. [PubMed: 20934413]

[47]. Bundy JL, Vied C, Nowakowski RS (2017) Sex differences in the molecular signature of the developing mouse hippocampus. BMC Genomics 18, 237. [PubMed: 28302071]

[48]. Leng S, Xue QL, Huang Y, Semba R, Chaves P, Bandeen-Roche K, Fried L, Walston J (2005) Total and differential white blood cell counts and their associations with circulating interleukin-6 levels in community-dwelling older women. J Gerontol A Biol Sci Med Sci 60, 195–199. [PubMed: 15814862]

[49]. Roubenoff R, Harris TB, Abad LW, Wilson PW, Dallal GE, Dinarello CA (1998) Monocyte cytokine production in an elderly population: effect of age and inflammation. J Gerontol A Biol Sci Med Sci 53, M20–26. [PubMed: 9467429]

[50]. Tan ZS, Beiser AS, Vasan RS, Roubenoff R, Dinarello CA, Harris TB, Benjamin EJ, Au R, Kiel DP, Wolf PA, Seshadri S (2007) Inflammatory markers and the risk of Alzheimer disease: the Framingham Study. Neurology 68, 1902–1908. [PubMed: 17536046]

[51]. Niraula A, Sheridan JF, Godbout JP (2017) Microglia Priming with Aging and Stress. Neuropsychopharmacology 42, 318–333. [PubMed: 27604565]

[52]. Tegeler C, O'Sullivan JL, Bucholtz N, Goldeck D, Pawelec G, Steinhagen-Thiessen E, Demuth I (2016) The inflammatory markers CRP, IL-6, and IL-10 are associated with cognitive function--data from the Berlin Aging Study II. Neurobiol Aging 38, 112–117. [PubMed: 26827649]

[53]. Lasselin J, Lekander M, Axelsson J, Karshikoff B (2018) Sex differences in how inflammation affects behavior: What we can learn from experimental inflammatory models in humans. Front Neuroendocrinol 50, 91–106. [PubMed: 29935190]

[54]. Galimberti D, Schoonenboom N, Scheltens P, Fenoglio C, Bouwman F, Venturelli E, Guidi I, Blankenstein MA, Bresolin N, Scarpini E (2006) Intrathecal chemokine synthesis in mild cognitive impairment and Alzheimer disease. Arch Neurol 63, 538–543. [PubMed: 16606766]

[55]. Galimberti D, Schoonenboom N, Scarpini E, Scheltens P, Dutch-Italian Alzheimer Research G (2003) Chemokines in serum and cerebrospinal fluid of Alzheimer's disease patients. Ann Neurol 53, 547–548. [PubMed: 12666129]

[56]. Duan RS, Yang X, Chen ZG, Lu MO, Morris C, Winblad B, Zhu J (2008) Decreased fractalkine and increased IP-10 expression in aged brain of APP(swe) transgenic mice. Neurochem Res 33, 1085–1089. [PubMed: 18095157]

[57]. Galimberti D, Fenoglio C, Lovati C, Venturelli E, Guidi I, Corra B, Scalabrini D, Clerici F, Mariani C, Bresolin N, Scarpini E (2006) Serum MCP-1 levels are increased in mild cognitive impairment and mild Alzheimer's disease. Neurobiol Aging 27, 1763–1768. [PubMed: 16307829]

[58]. Prinz M, Priller J (2010) Tickets to the brain: role of CCR2 and CX3CR1 in myeloid cell entry in the CNS. J Neuroimmunol 224, 80–84. [PubMed: 20554025]

[59]. Stalder AK, Ermini F, Bondolfi L, Krenger W, Burbach GJ, Deller T, Coomaraswamy J, Staufenbiel M, Landmann R, Jucker M (2005) Invasion of hematopoietic cells into the brain of amyloid precursor protein transgenic mice. J Neurosci 25, 11125–11132. [PubMed: 16319312]

[60]. Wang Y, Ulland TK, Ulrich JD, Song W, Tzaferis JA, Hole JT, Yuan P, Mahan TE, Shi Y, Gilfillan S, Cella M, Grutzendler J, DeMattos RB, Cirrito JR, Holtzman DM, Colonna M (2016) TREM2-mediated early microglial response limits diffusion and toxicity of amyloid plaques. J Exp Med 213, 667–675. [PubMed: 27091843]

[61]. Naert G, Rivest S (2011) CC chemokine receptor 2 deficiency aggravates cognitive impairments and amyloid pathology in a transgenic mouse model of Alzheimer's disease. J Neurosci 31, 6208–6220. [PubMed: 21508244]

[62]. Prokop S, Miller KR, Drost N, Handrick S, Mathur V, Luo J, Wegner A, Wyss-Coray T, Heppner FL (2015) Impact of peripheral myeloid cells on amyloid-beta pathology in Alzheimer's disease-like mice. J Exp Med 212, 1811–1818. [PubMed: 26458768]

[63]. Griffin WS (2011) Alzheimer's - Looking beyond plaques. F1000 Med Rep 3, 24. [PubMed: 22162727]

[64]. Ghosh S, Wu MD, Shaftel SS, Kyrkanides S, LaFerla FM, Olschowka JA, O'Banion MK (2013) Sustained interleukin-1beta overexpression exacerbates tau pathology despite reduced amyloid burden in an Alzheimer's mouse model. J Neurosci 33, 5053–5064. [PubMed: 23486975]

[65]. Maphis N, Xu G, Kokiko-Cochran ON, Jiang S, Cardona A, Ransohoff RM, Lamb BT, Bhaskar K (2015) Reactive microglia drive tau pathology and contribute to the spreading of pathological tau in the brain. Brain 138, 1738–1755. [PubMed: 25833819]

[66]. Heneka MT, Kummer MP, Stutz A, Delekate A, Schwartz S, Vieira-Saecker A, Griep A, Axt D, Remus A, Tzeng TC, Gelpi E, Halle A, Korte M, Latz E, Golenbock DT (2012) NLRP3 is activated in Alzheimer's disease and contributes to pathology in APP/PS1 mice. Nature.

[67]. Steinman L (2013) Inflammatory cytokines at the summits of pathological signal cascades in brain diseases. Sci Signal 6, pe3. [PubMed: 23322904]

[68]. Swardfager W, Lanctot K, Rothenburg L, Wong A, Cappell J, Herrmann N (2010) A meta-analysis of cytokines in Alzheimer's disease. Biol Psychiatry 68, 930–941. [PubMed: 20692646]

[69]. MacPherson KP, Sompol P, Kannarkat GT, Chang J, Sniffen L, Wildner ME, Norris CM, Tansey MG (2017) Peripheral administration of the soluble TNF inhibitor XPro1595 modifies brain immune cell profiles, decreases beta-amyloid plaque load, and rescues impaired long-term potentiation in 5xFAD mice. Neurobiol Dis 102, 81–95. [PubMed: 28237313]

[70]. Oka A, Takashima S (1997) Induction of cyclo-oxygenase 2 in brains of patients with Down's syndrome and dementia of Alzheimer type: specific localization in affected neurones and axons. Neuroreport 8, 1161–1164. [PubMed: 9175105]

[71]. Pasinetti GM, Aisen PS (1998) Cyclooxygenase-2 expression is increased in frontal cortex of Alzheimer's disease brain. Neuroscience 87, 319–324. [PubMed: 9740394]

[72]. Hoozemans JJ, van Haastert ES, Veerhuis R, Arendt T, Scheper W, Eikelenboom P, Rozemuller AJ (2005) Maximal COX-2 and ppRb expression in neurons occurs during early Braak stages prior to the maximal activation of astrocytes and microglia in Alzheimer's disease. J Neuroinflammation 2, 27. [PubMed: 16300681]

[73]. Rojas A, Ganesh T, Lelutiu N, Gueorguieva P, Dingledine R (2015) Inhibition of the prostaglandin EP2 receptor is neuroprotective and accelerates functional recovery in a rat model of organophosphorus induced status epilepticus. Neuropharmacology 93, 15–27. [PubMed: 25656476]

[74]. Jiang J, Quan Y, Ganesh T, Pouliot WA, Dudek FE, Dingledine R (2013) Inhibition of the prostaglandin receptor EP2 following status epilepticus reduces delayed mortality and brain inflammation. Proc Natl Acad Sci U S A.

[75]. Jiang J, Quan Y, Ganesh T, Pouliot WA, Dudek FE, Dingledine R (2013) Inhibition of the prostaglandin receptor EP2 following status epilepticus reduces delayed mortality and brain inflammation. Proc Natl Acad Sci U S A 110, 3591–3596. [PubMed: 23401547]

[76]. Serrano GE, Lelutiu N, Rojas A, Cochi S, Shaw R, Makinson CD, Wang D, FitzGerald GA, Dingledine R (2011) Ablation of cyclooxygenase-2 in forebrain neurons is neuroprotective and dampens brain inflammation after status epilepticus. J Neurosci 31, 14850–14860. [PubMed: 22016518]

[77]. Radde R, Bolmont T, Kaeser SA, Coomaraswamy J, Lindau D, Stoltze L, Calhoun ME, Jaggi F, Wolburg H, Gengler S, Haass C, Ghetti B, Czech C, Holscher C, Mathews PM, Jucker M (2006) Abeta42-driven cerebral amyloidosis in transgenic mice reveals early and robust pathology. EMBO Rep 7, 940–946. [PubMed: 16906128]

[78]. Sturchler-Pierrat C, Abramowski D, Duke M, Wiederhold KH, Mistl C, Rothacher S, Ledermann B, Burki K, Frey P, Paganetti PA, Waridel C, Calhoun ME, Jucker M, Probst A, Staufenbiel M, Sommer B (1997) Two amyloid precursor protein transgenic mouse models with Alzheimer disease-like pathology Proc Natl Acad Sci U S A 94, 13287–13292. [PubMed: 9371838]

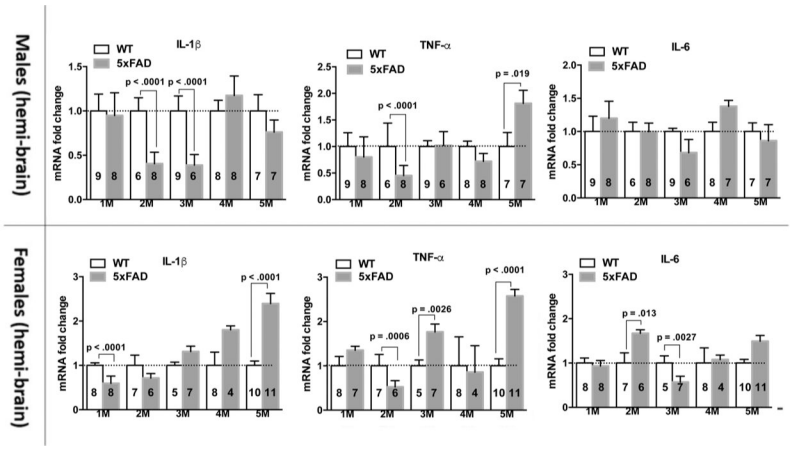

Figure 1:

mRNA expression levels of pro-inflammatory genes in the hemi-brain of male and female 5xFAD mice and wild-type littermates from 1–5 months. Data were analyzed by two-way ANOVA with Sidak's multiple comparison test using ΔΔCT values. The number of mice analyzed in each group is noted in the bar. Data represent the mean ± SEM.

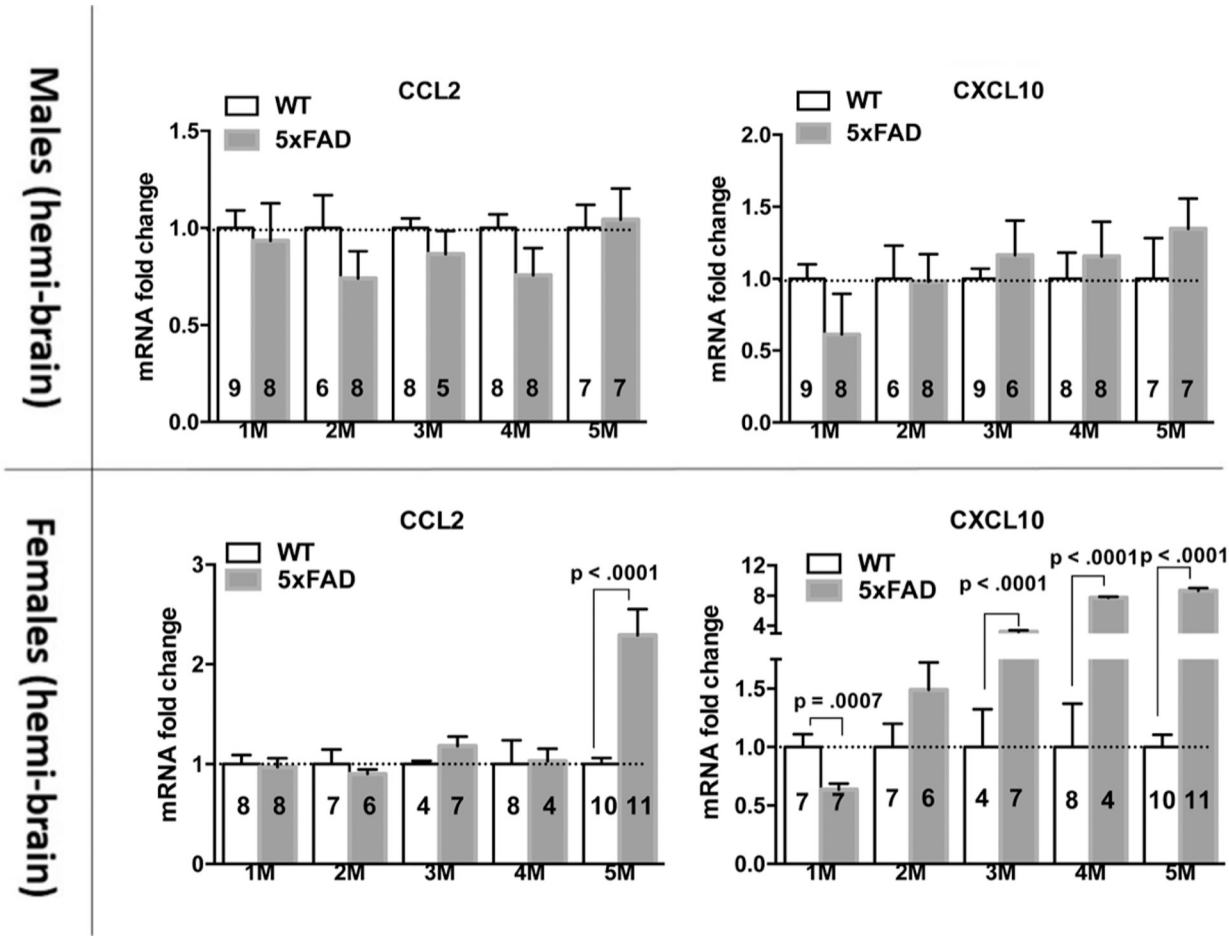

Figure 2:

mRNA expression of chemokines CCL2 and CXCL10 in the 5xFAD mice and wild- type littermates from 1–5 months of age. Two-way ANOVA with Sidak's multiple comparison test using ΔΔCT values. The number of mice analyzed in each group is noted in the bar. Data represent the mean ± SEM.

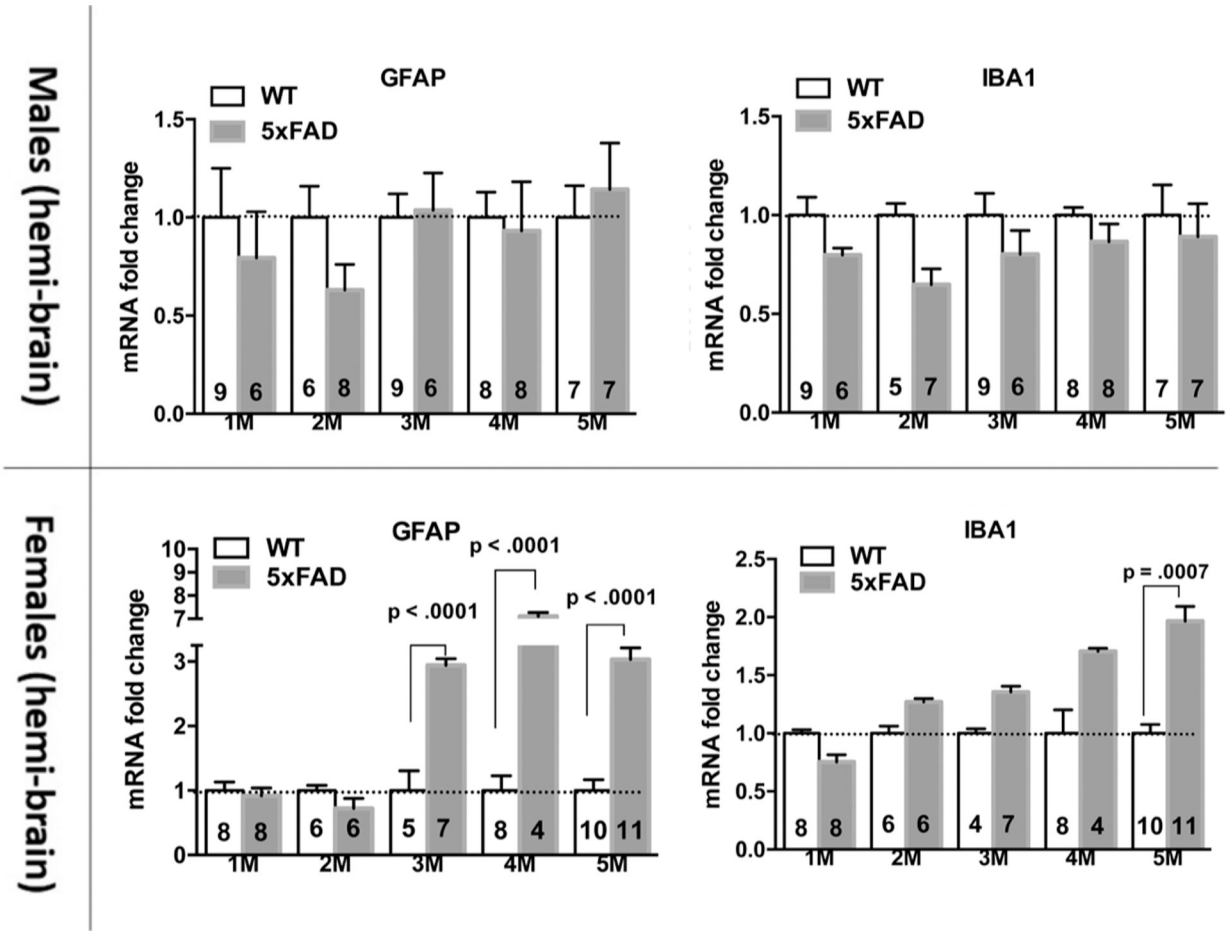

Figure 3:

mRNA expression of glial cell markers in the hemi-brain of 5xFAD and non-transgenic mice from 1–5 months of age. Two-way ANOVA with Sidak's multiple comparison test using ΔΔCT values. The number of mice analyzed in each group is noted in the bar. Data represent the mean ± SEM.

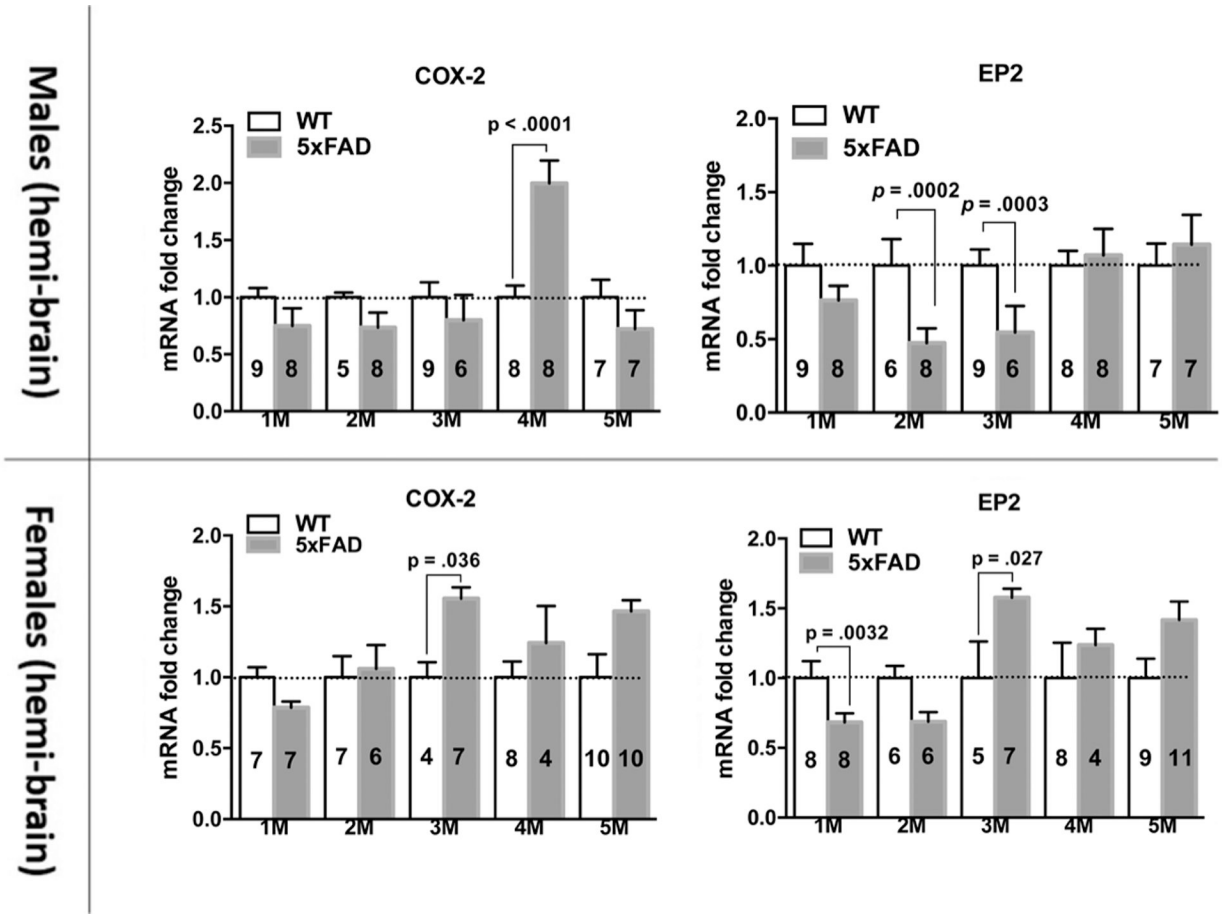

Figure 4:

mRNA expression of COX-2 and EP2 in the hemi-brain of 5xFAD and non-transgenic mice from 1–5 months of age. Two-way ANOVA with Sidak's multiple comparison test using ΔΔCT values. The number of mice analyzed in each group is noted in the bar. Data represent the mean ± SEM.

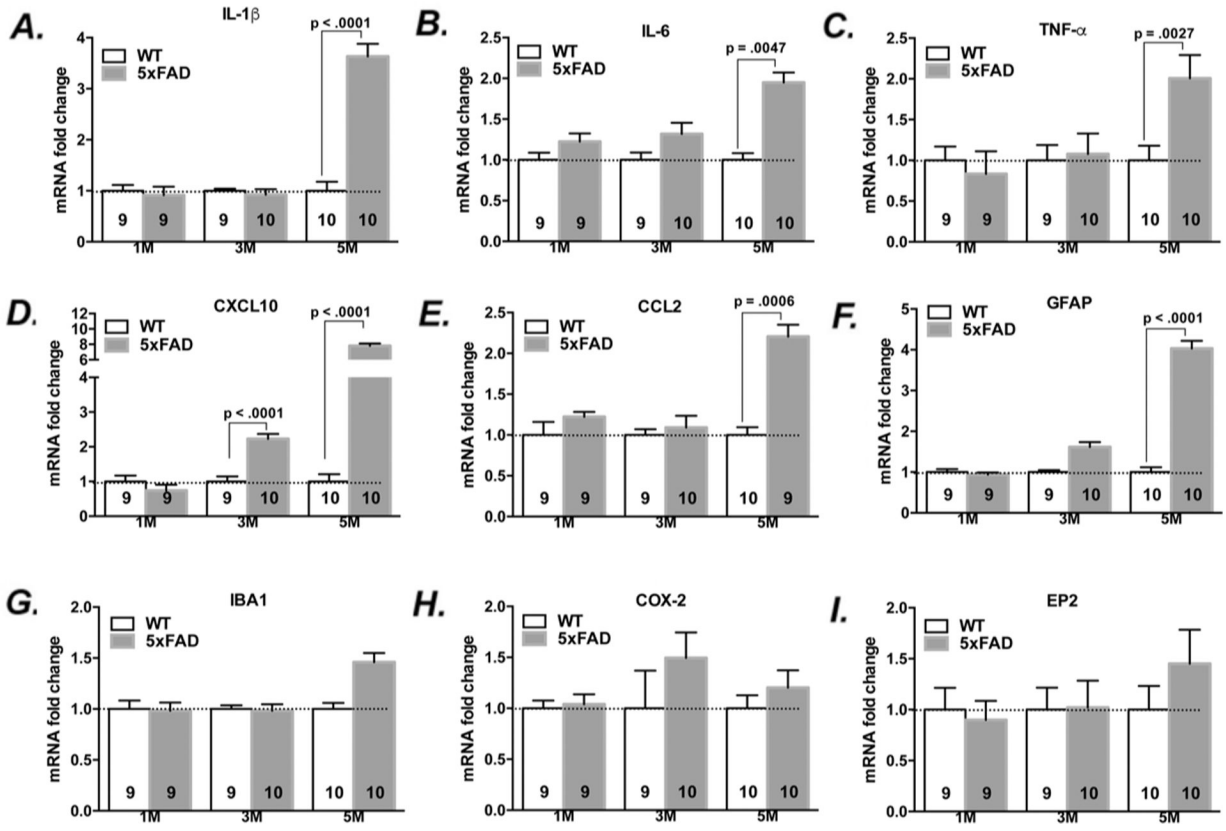

Figure 5:

mRNA expression of inflammatory mediators and glial markers in the cortices of female 5xFAD and non-transgenic mice at one, three, and five months of age. Two-way ANOVA with Sidak's multiple comparison test using ΔΔCT values. The number of mice analyzed in each group is noted in the bar. Data represent the mean ± SEM.

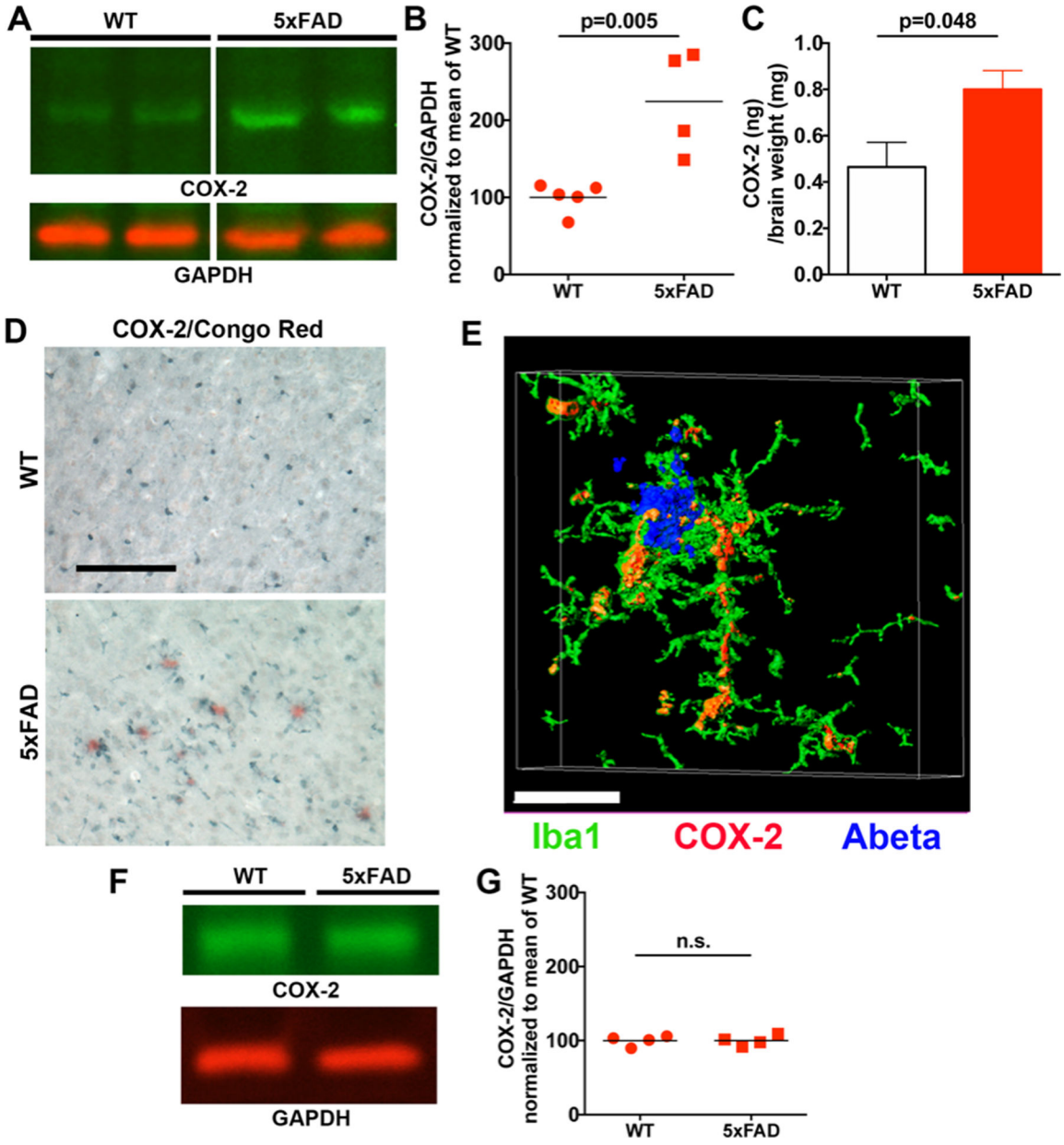

Figure 6.

Cortical COX-2 levels are elevated in female, but not male, 5xFAD mice. (A) COX-2 protein levels in cortical homogenates of five-month-old female control wild-type and 5xFAD mice were measured by Western blot with GAPDH as loading control. Two representative samples from each genotype are shown. The images were cropped from the same blot for clarity. (B) Normalized band intensity of the COX-2 protein relative to that of GAPDH and referenced to the mean COX-2/GAPDH ratio in female wild-type (n=5) and 5xFAD (n=4) mice. The symbols represent each individual mouse and the horizontal line represents the mean value. The mean ratio was compared by a Student's *t*-test. (C) ELISA revealed elevated COX-2 levels in cortical homogenates from five-month-old 5xFAD mice compared to wild-type controls. The average COX-2 levels were compared by a Student's *t*-test. (D)

Histological examination shows COX-2-immunoreactive cells tiled throughout the cortex of wild-type mice (left panel). The COX-2-expressing cells were found clustered around congophillic Aβ deposits in 5xFAD mice aged to five months of age (right panel). COX-2-immunoreactive cells were also observed at distance from Aβ deposits, tiled throughout the cortex. Scale bar = 50 μm. (E) Three-dimensional surface area reconstruction of COX-2 (red) with Iba1-expressing cortical myeloid cells (green) in the vicinity of Aβ deposits (blue). The orange color represents co-localization between COX-2 (red) and Iba-1 (green) staining. Scale bar is 15 μm. (F) COX-2 protein levels in cortical homogenates of five-month-old male control wild-type and 5xFAD mice were measured by Western blot with GAPDH as loading control. A representative sample from each genotype is shown. (G) Normalized band intensity of the COX-2 protein relative to that of GAPDH and referenced to the mean COX-2/GAPDH ratio in male wild-type (n=4) and 5xFAD (n=4) mice. The symbols represent each individual mouse and the horizontal line represents the mean value. The mean ratio was compared by a Student's *t*-test.

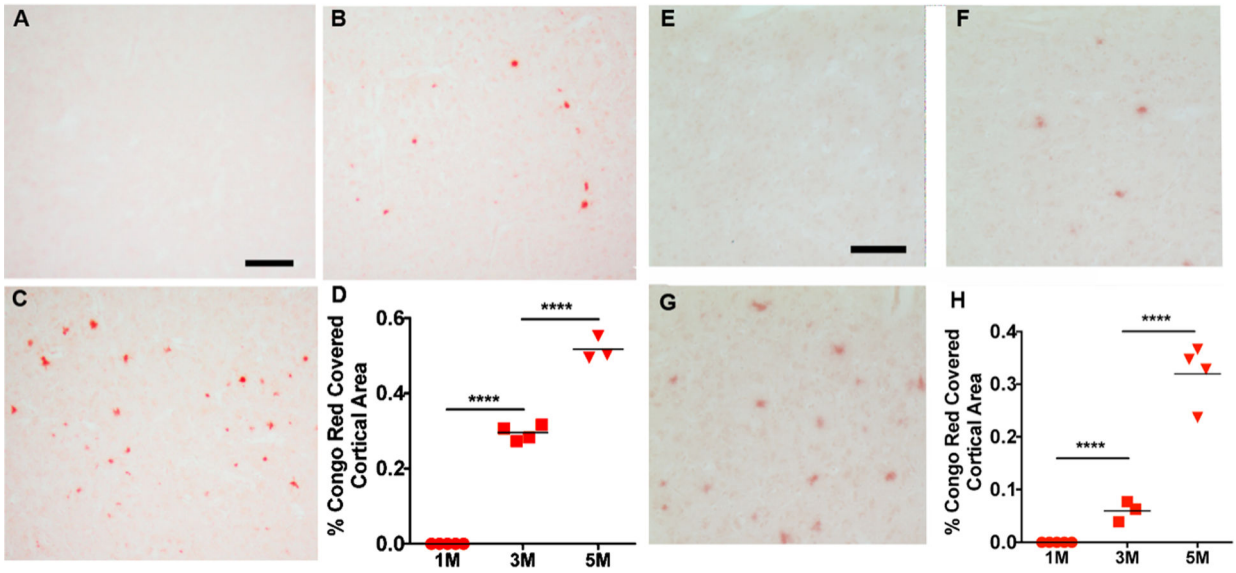

Figure 7.

Age-dependent increase in cortical dense-core Aβ deposition. Cortical brain tissue sections from (A) one-, (B) three-, and (C) five-month-old female 5xFAD mice were stained with Congo red to label dense-core congophilic Aβ deposits. (D) Stereological quantification of congophilic Aβ deposits at one-, three-, and five-months of age revealed an age-dependent increase in cortical area covered by congophilic Aβ deposition. The mean area covered by Congo red staining in four cortical brain sections per mouse was determined. Each symbol represents the mean value from four non-adjacent sections per mouse (1M: n=5 mice, 3M: n=4 mice, and 5M: n=3 mice). Tissues from male 5xFAD mice aged to (E) one-, (F) three-, and (G) five-month-old were also stained with Congo red. (H) Stereological quantification of congophilic Aβ deposits revealed an age-dependent increase in cortical area covered by congophilic Aβ deposition. The mean area covered by Congo red staining in six cortical brain sections per mouse was determined. Each symbol represents the mean value from four non-adjacent sections per mouse (1M: n=5 mice, 3M: n=3 mice, and 5M: n=4 mice). One-way ANOVA with Sidak's multiple comparison test revealed a significant difference between each age, ****= $p<0.0001$. Scale bar is 50 μm in A, B, and C and 25 μm in E, F, and G.

Table 1.

Real Time PCR mouse primer sequences. The approved human gene nomenclature symbol is in parentheses if different from gene name.

Genes	Forward Primer (sequence 5'−3')	Reverse Primer (sequence 5'−3')
GAPDH	TGTCCGTCGTGGATCTGAC	CCTGCTTCACCACCTTCTTG
COX-2 (PTGS2)	ACCAACGCTGCCACAACT	GGTTGGAACAGCAAGGATTT
TNF-α (TNF)	TCTTCTGTCTACTGAACTTCGG	AAGATGATCTGAGTGTGAGGG
IL-1β (IL1B)	CAGGAAGGCAGTGTCACTCA	TCCCACGAGTCACAGAGGA
CXCL10	GTGCTGCTGAGTCTGAGTGG	TTGCAGGAATGATTTCAAGTTTT
CCL2	CATCCACGTGTTGGCTCA	GCTGCTGGTGATCCTCTTGTA
IL-6 (IL6)	AACTCCATCTGCCCTTCAGGAACA	AAGGCAGTGGCTGTCAACAACATC
GFAP	GACAACTTTGCACAGGACCTC	ATACGCAGCCAGGTTGTTCT
Iba1 (AIF1)	GGATTTGCAGGGAGGAAAAG	TGGGATCATCGAGGAATTG
EP2 (PTGER2)	TCTTTAGTCTGGCCACGATGCTCA	GCAGGGAACAGAAGAGCAAGGAGG